

Non-relativistic limit of multidimensional gravity: exact solutions and applications

Maxim Eingorn[†], Alexander Zhuk[‡]

Astronomical Observatory and Department of Theoretical Physics, Odessa
National University, Street Dvoryanskaya 2, Odessa 65082, Ukraine

Abstract. It is found the exact solution of the Poisson equation for the multidimensional space with topology $M_{3+d} = \mathbb{R}^3 \times T^d$. This solution describes smooth transition from the newtonian behavior $1/r_3$ for distances bigger than periods of tori (the extra dimension sizes) to multidimensional behavior $1/r_{3+d}^{1+d}$ in opposite limit. In the case of one extra dimension $d = 1$, the gravitational potential is expressed via compact and elegant formula. These exact solutions are applied to some practical problems to get the gravitational potentials for considered configurations. Found potentials are used to calculate the acceleration for point masses and gravitational self-energy. It is proposed models where the test masses are smeared over some (or all) extra dimensions. In 10-dimensional spacetime with 3 smeared extra dimensions, it is shown that the size of 3 rest extra dimensions can be enlarged up to submillimeter for the case of 1TeV fundamental Planck scale $M_{Pl(10)}$. In the models where all extra dimensions are smeared, the gravitational potential exactly coincides with the newtonian one regardless of size of the extra dimensions. Nevertheless, the hierarchy problem can be solved in these models.

PACS numbers: 04.50.-h, 11.25.Mj, 98.80.-k

[†] e-mail: maxim.eingorn@gmail.com

[‡] e-mail: ai_zhuk2@rambler.ru

1. Introduction

There are two well-known problems which are related to each other. They are the discrepancies in gravitational constant experimental data and the hierarchy problem. Discrepancies (see e.g. Figure 2 in the "CODATA Recommended Values of the Fundamental Constants: 2006") are usually explained by extreme weakness of gravity. It is very difficult to measure the Newton's gravitational constant G_N . Certainly, for this reason geometry of an experimental setup can effect on data. However, it may well be that, the discrepancies can also be explained (at least partly) by underlying fundamental theory. Formulas for an effective gravitational constant following from such theory can be sensitive to the geometry of experiments. For example, if correction to the Newton's gravitational potential has the form of Yukawa potential, then the force due to this potential at a given minimum separation per unit test-body mass is least for two spheres and greatest for two planes (see e.g. [1]). Therefore, an effective gravitational constant obtained from these formulas acquires different values for different experimental setup.

The hierarchy problem - the huge gap between the electroweak scale $M_{EW} \sim 10^3 \text{GeV}$ and the Planck scale $M_{Pl(4)} = 1.2 \times 10^{19} \text{GeV}$ - can be also reformulated in the following manner: why is gravity so weak? The smallness of G_N is the result of relation $G_N = M_{Pl(4)}^{-2}$ and huge value of $M_{Pl(4)}$. The natural explanation was proposed in [2, 3]: the gravity is strong: $G_{\mathcal{D}} = M_{Pl(\mathcal{D})}^{-(2+d)} \sim M_{EW}^{-(2+d)}$ and it happens in $(\mathcal{D} = 4 + d)$ -dimensional spacetime. It becomes weak when gravity is "smeared" over large extra dimensions: $G_N \sim G_{\mathcal{D}}/V_d$ where V_d is a volume of internal space.

To shed light on both of these problems from new standpoint we intend to investigate multidimensional gravity in non-relativistic limit. To do that, first, we are going to obtain a solution of $(D = 3 + d)$ -dimensional Poisson equation in the case of toroidal extra dimensions. From school years we know that newtonian gravitational potential of a body with mass m has the form of $\varphi(r_3) = -G_N m/r_3$ where G_N is Newton's gravitational constant and $r_3 = |\mathbf{r}_3|$ is magnitude of a radius vector in three-dimensional space. This expression is the solution of three-dimensional Poisson equation with a point-mass source (and corresponding boundary condition $\varphi(r_3) \rightarrow 0$ for $r_3 \rightarrow +\infty$) or it can be derived from Gauss's flux theorem in three-dimensional space. To investigate effects of extra dimensions, it is necessary to generalize the Newton's formula to the case of extra dimensions. Clearly, the result depends on topology of investigated models. We consider models where D -dimensional spatial part of factorizable geometry is defined on a product manifold $M_D = \mathbb{R}^3 \times T^d$. \mathbb{R}^3 describes three-dimensional flat external (our) space and T^d is a torus which corresponds to d -dimensional internal space. Let V_d be a volume of the internal space and $a \sim V_d^{1/d}$ is a characteristic size of extra dimensions. Then, Gauss's flux theorem leads to the following asymptotes for gravitational potential (see e.g. [3] and our Appendix for alternative derivation): $\varphi \sim 1/r_3$ for $r_3 \gg a$ and $\varphi \sim 1/r_{3+d}^{1+d}$ for $r_{3+d} \ll a$ where r_3 and r_{3+d} are magnitudes of radius vectors in three-dimensional and $(3+d)$ -dimensional spaces, respectively. Obviously, an exact solution of D -dimensional Poisson equation should show smooth transition between both of these asymptotes. This formula gives possibility to investigate characteristic features of multidimensional gravity in non-relativistic limit which enable us to reveal extra dimensions (or to establish experimental limitations on extra dimensions).

In our paper we obtain such exact solution for arbitrary number of the extra

dimensions. In the case of one extra dimension, this expression acquires very compact and elegant form. Found exact solution is applied to a number of practical problems, e.g. to calculate gravitational force between two spherical shells (or balls). It gives a possibility to calculate an effective four-dimensional gravitational constant for given configurations. For example, in the case of two balls we show that, in principle, the inverse square law experiments enable us to detect a deviation from the Newton's gravitational constant. Then, we generalize our model to the case of smeared extra dimensions. It means that we suppose that test bodies are uniformly smeared/spreaded over all or part of extra dimensions. We prove that the gravitational potential does not feel the smeared extra dimensions. In particular, if all extra dimensions are smeared, then the inverse square law experiment does not show any deviation from the ordinary Newton's formula, and this conclusion does not depend on sizes of the smeared extra dimensions. Nevertheless, the hierarchy problem can be solved in these models.

The paper is structured as follows. In section 2 we get the exact solution of multidimensional Poisson equation in the case of spacial topology $\mathbb{R}^3 \times T^d$. This formula is applied to some practical problems in section 3 to get gravitational potential, gravitational acceleration of a point mass and gravitational self-energy for these problems. In section 4 we investigate gravitational interaction of two spherical shells. Then, in section 5 we generalize our model to the case of smeared extra dimensions. Here, we prove that gravitational potential does not "feel" the smeared extra dimensions and demonstrate that the hierarchy problem can be solved in this case. A brief discussion of the obtained results is presented in the concluding section 6. In Appendix A, we get the expressions for the gravitational force law at small and big separation between point masses on multidimensional manifold with topology $\mathbb{R}^3 \times T^d$.

2. Multidimensional gravitational potentials

In D -dimensional space, the Poisson equation reads

$$\Delta_D \varphi_D = S_D G_D \rho_D(\mathbf{r}_D), \quad (2.1)$$

where $S_D = 2\pi^{D/2}/\Gamma(D/2)$ is a total solid angle (square of $(D-1)$ -dimensional sphere of a unit radius), G_D is a gravitational constant in $(\mathcal{D} = D+1)$ -dimensional spacetime and $\rho_D(\mathbf{r}_D) = m\delta(x_1)\delta(x_2)\dots\delta(x_D)$.

2.1. Spatial topology \mathbb{R}^D

In the case of topology \mathbb{R}^D , (2.1) has the following solution:

$$\varphi_D(\mathbf{r}_D) = -\frac{G_D m}{(D-2)r_D^{D-2}}, \quad D \geq 3. \quad (2.2)$$

This is the unique solution of (2.1) which satisfies the boundary condition: $\lim_{r_D \rightarrow +\infty} \varphi_D(\mathbf{r}_D) = 0$. Gravitational constant G_D in (2.1) is normalized in such a way that the strength of gravitational field (acceleration of a test body) takes the form: $-d\varphi_D/dr_D = -G_D m/r_D^{D-1}$.

2.2. Spatial topology $\mathbb{R}^3 \times T^d$, d -arbitrary

If topology of space is $\mathbb{R}^3 \times T^d$, then it is natural to impose periodic boundary conditions in the directions of the extra dimensions: $\varphi_D(\mathbf{r}_3, \xi_1, \xi_2, \dots, \xi_i, \dots, \xi_d) = \varphi_D(\mathbf{r}_3, \xi_1, \xi_2, \dots, \xi_i + a_i, \dots, \xi_d)$, $i = 1, \dots, d$, where a_i denotes a period in the direction of the extra dimension ξ_i . Then, Poisson equation has solution (cf. also with [3, 4]):

$$\begin{aligned} \varphi_D(\mathbf{r}_3, \xi_1, \dots, \xi_d) = & -\frac{G_N m}{r_3} \\ & \times \sum_{k_1=-\infty}^{+\infty} \dots \sum_{k_d=-\infty}^{+\infty} \exp \left[-2\pi \left(\sum_{i=1}^d \left(\frac{k_i}{a_i} \right)^2 \right)^{1/2} r_3 \right] \\ & \times \cos \left(\frac{2\pi k_1}{a_1} \xi_1 \right) \dots \cos \left(\frac{2\pi k_d}{a_d} \xi_d \right). \end{aligned} \quad (2.3)$$

To get this result we, first, use the formula $\delta(\xi_i) = \frac{1}{a_i} \sum_{k=-\infty}^{+\infty} \cos \left(\frac{2\pi k}{a_i} \xi_i \right)$ and, second, put the following relation between gravitational constants in four- and \mathcal{D} -dimensional spacetimes:

$$\frac{S_D}{S_3} \cdot \frac{G_D}{\prod_{i=1}^d a_i} = G_N. \quad (2.4)$$

The latter relation provides correct limit when all $a_i \rightarrow 0$. In this limit zero modes $k_i = 0$ give the main contribution and we obtain $\varphi_D(\mathbf{r}_3, \xi_1, \dots, \xi_d) \rightarrow -G_N m / r_3$. (2.4) was widely used in the concept of large extra dimensions which gives possibility to solve the hierarchy problem [2, 3]. It is also convenient to rewrite (2.4) via fundamental Planck scales:

$$\frac{S_D}{S_3} \cdot M_{Pl(4)}^2 = M_{Pl(\mathcal{D})}^{2+d} \prod_{i=1}^d a_i, \quad (2.5)$$

where $M_{Pl(4)} = G_N^{-1/2} = 1.2 \times 10^{19} \text{ GeV}$ and $M_{Pl(\mathcal{D})} \equiv G_{\mathcal{D}}^{-1/(2+d)}$ are fundamental Planck scales in four and \mathcal{D} spacetime dimensions, respectively.

In opposite limit when all $a_i \rightarrow +\infty$ the sums in (2.3) can be replaced by integrals. Using the standard integrals (e.g. from [5]) and relation (2.4), we can easily show that, for example, in particular cases $d = 1, 2$ we get desire result: $\varphi_D(\mathbf{r}_3, \xi_1, \dots, \xi_d) \rightarrow -G_D m / [(D-2) r_{3+d}^{1+d}]$.

From (2.3), it follows that potential energy of gravitational interaction between two point masses $m^{(a)}$ and $m^{(b)}$ with radius vectors $\mathbf{r}_D^{(a)}$ and $\mathbf{r}_D^{(b)}$ reads

$$\begin{aligned} U_D(\mathbf{r}_D^{(a)}, \mathbf{r}_D^{(b)}) = & -\frac{G_N m^{(a)} m^{(b)}}{|\mathbf{r}_3^{(a)} - \mathbf{r}_3^{(b)}|} \\ & \times \sum_{k_1=-\infty}^{+\infty} \dots \sum_{k_{D-3}=-\infty}^{+\infty} \exp \left[-2\pi \left(\sum_{i=1}^{D-3} \left(\frac{k_i}{a_i} \right)^2 \right)^{1/2} |\mathbf{r}_3^{(a)} - \mathbf{r}_3^{(b)}| \right] \\ & \times \cos \left(\frac{2\pi k_1}{a_1} |\xi_1^{(a)} - \xi_1^{(b)}| \right) \dots \cos \left(\frac{2\pi k_{D-3}}{a_{D-3}} |\xi_{D-3}^{(a)} - \xi_{D-3}^{(b)}| \right). \end{aligned} \quad (2.6)$$

2.3. Spatial topology $\mathbb{R}^3 \times T^1$

In the case of one extra dimension $d = 1$ we can perform summation of series in (2.3). To do it, we can apply the Abel-Plana formula or simply use the tables of series [5]. As a result, we arrive at compact and nice expression:

$$\varphi_4(\mathbf{r}_3, \xi) = -\frac{G_N m}{r_3} \frac{\sinh\left(\frac{2\pi r_3}{a}\right)}{\cosh\left(\frac{2\pi r_3}{a}\right) - \cos\left(\frac{2\pi \xi}{a}\right)}, \quad (2.7)$$

where $r_3 \in [0, +\infty)$ and $\xi \in [0, a]$. It is not difficult to verify that this formula has correct asymptotes when $r_3 \gg a$ and $r_4 \ll a$. Figure 1 demonstrates the shape of this potential. Dimensionless variables $\eta_1 \equiv r_3/a \in [0, +\infty)$ and $\eta_2 \equiv \xi/a \in [0, 1]$. With respect to variable η_2 , this potential has two minima at $\eta_2 = 0, 1$ and one maximum at $\eta_2 = 1/2$. We continue the graph to negative values of $\eta_2 \in [-1, 1]$ to show in more detail the form of minimum at $\eta_2 = 0$. The potential (2.7) is finite for any value of r_3 if $\xi \neq 0, a$ and goes to $-\infty$ as $-1/r_4^2$ if simultaneously $r_3 \rightarrow 0$ and $\xi \rightarrow 0, a$ (see Figure 2). We would like to mention that in particular case $\xi = 0$ formula (2.7) was also found in [6].

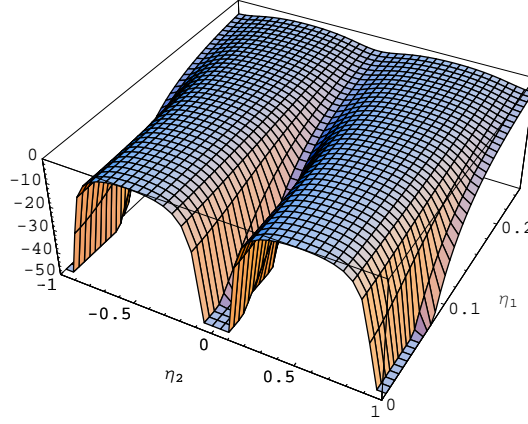


Figure 1. Graph of function $\tilde{\varphi}(\eta_1, \eta_2) \equiv \varphi_4(\mathbf{r}_3, \xi)/(G_N m/a) = -\sinh(2\pi\eta_1)/[\eta_1(\cosh(2\pi\eta_1) - \cos(2\pi\eta_2))]$.

2.4. Yukawa approximation

Having at hand formulas (2.3) and (2.7), we can apply it for calculation of some elementary physical problems and compare obtained results with known newtonian expressions. For a working approximation, it is usually sufficient to summarize in (2.3) up to the first Kaluza-Klein modes $|k_i| = 1$ ($i = 1, \dots, d$):

$$\varphi_D(\mathbf{r}_3, \xi_1, \xi_2, \dots, \xi_d) \approx -\frac{G_N m}{r_3} \left[1 + 2 \sum_{i=1}^d \exp\left(-\frac{2\pi}{a_i} r_3\right) \cos\left(\frac{2\pi}{a_i} \xi_i\right) \right]. \quad (2.8)$$

Then, the terms with the biggest periods a_i give the main contributions. If all test bodies are on the same brane ($\xi_i = 0$) we obtain:

$$\varphi_D(\mathbf{r}_3, \xi_1 = 0, \xi_2 = 0, \dots, \xi_d = 0) \equiv \varphi_D(r_3) \approx -\frac{G_N m}{r_3} \left[1 + \alpha \exp\left(-\frac{r_3}{\lambda}\right) \right], \quad (2.9)$$

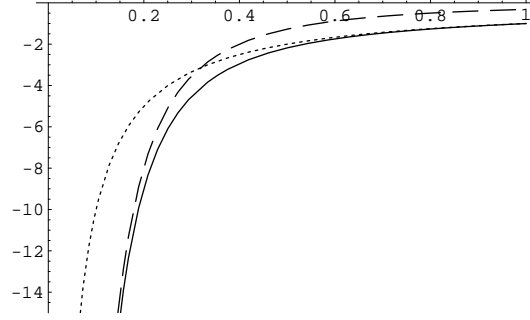


Figure 2. Section $\xi = 0$ of potential (2.7). Solid line is $\tilde{\varphi}(\eta_1, 0) = -\sinh(2\pi\eta_1)/[\eta_1(\cosh(2\pi\eta_1)-1)]$ which goes to $-1/\eta_1$ (dotted line) for $\eta_1 \rightarrow +\infty$ and to $-1/(\pi\eta_1^2)$ (dashed line) for $\eta_1 \rightarrow 0$.

where $\alpha = 2s$ ($1 \leq s \leq d$), $\lambda = a/(2\pi)$ and s is a number of extra dimensions with periods of tori a_i which are equal (or approximately equal) to $a = \max a_i$. If $a_1 = a_2 = \dots = a_d = a$, then $s = d$. Thus, the correction to Newton's potential has the form of Yukawa potential. It is now customary to interpret tests of gravitational inverse-square law (ISL) as setting limits on additional Yukawa contribution. The overall diagram of the experimental constraints can be found in [7] (see Figure 6) and we shall use these data for limitation a for given α .

3. Application ($\xi_i = 0$)

Now, we apply formulas (2.3) and (2.7) to some particular geometrical configurations. For our calculations we shall use the case of $\xi_1 = \xi_2 = \dots = \xi_d = 0$. It means that test bodies have the same coordinates in the extra dimension. It takes place e.g. when test bodies are on the same brane. Also, to get numerical results we should define the sizes a_i of the extra dimensions. The e^+e^- leptonic interaction experiments at high-energy colliders show that there is no deviations from Coulomb's law for separations down to 10^{-16}cm [1]. Therefore, if the standard model fields are not localized on the brane, this value can be used for upper bound of a_i : $a_i \lesssim 10^{-17}\text{cm}$ (in section 5 we demonstrate how to avoid this argument). These values a_i can be greatly increased if we suppose that the standard model fields are localized on the brane. In this case, we can obtain the upper bound for $a = \max a_i$ from the gravitational inverse-square law experimental data depicted in Figure 6 of paper [7]. For example, the Yukawa approximation (2.9) shows that $\alpha = 2$ for $d = 1$. For this value α , Figure 6 gives $\lambda \leq 4.7 \times 10^{-3}\text{cm} \Rightarrow a \leq 3.0 \times 10^{-2}\text{cm}$.

3.1. Infinitesimally thin shell

Let us consider first an infinitesimally thin shell of mass $m = 4\pi R^2\sigma$, where R and σ are radius and surface density of the shell. Then, gravitational potential of this shell in a point with radius vector \mathbf{r}_3 (from the center of the shell) is

$$\varphi_D(r_3) = -\frac{2\pi G_N \sigma R}{r} \int_{r_3-R}^{r_3+R} \sum_k \exp[-2\pi\chi_k r'] dr' \quad (3.1)$$

$$= -\frac{G_N m}{r_3} - \frac{2G_N \sigma R}{r_3} \sum_k' \frac{1}{\chi_k} e^{-2\pi\chi_k r_3} \sinh(2\pi\chi_k R), \quad r_3 > R$$

and

$$\begin{aligned} \varphi_D(r_3) &= -\frac{2G_N \sigma R}{r_3} \int_{R-r_3}^{R+r_3} \sum_k \exp[-2\pi\chi_k r'] dr' \\ &= -\frac{G_N m}{R} - \frac{2G_N \sigma R}{r_3} \sum_k' \frac{1}{\chi_k} e^{-2\pi\chi_k R} \sinh(2\pi\chi_k r_3), \quad r_3 < R, \end{aligned} \quad (3.2)$$

where

$$\chi_k \equiv \left[\sum_{i=1}^d \left(\frac{k_i}{a_i} \right)^2 \right]^{1/2}, \quad \sum_k \equiv \sum_{k_1=-\infty}^{+\infty} \dots \sum_{k_d=-\infty}^{+\infty} \quad (3.3)$$

and the prime in sums denotes that the zero mode $k_1 = \dots = k_d = 0$ is absent in summation. It means that the Newton's expressions (which correspond to the zero mode) are singled out from sums. In the case $d = 1$, these expressions can be written in the compact form:

$$\varphi_4(r_3) = -\frac{G_N \sigma R a}{r_3} \ln \left\{ \frac{\cosh\left(\frac{2\pi(r_3+R)}{a}\right) - 1}{\cosh\left(\frac{2\pi(r_3-R)}{a}\right) - 1} \right\}, \quad r_3 \geq R. \quad (3.4)$$

These formulas demonstrate two features of the considered models. Firstly, we see that inside ($r_3 < R$) of the shell gravitational potential is not a constant. Thus, a test body undergoes an acceleration in contrast to the newtonian case (and to Birkhoff's theorem of general relativity in four-dimensional spacetime which states that the metric inside an empty spherical cavity in the center of a spherically symmetric system is the Minkowski metric). Secondly, if $r_3 \rightarrow R$, these potentials have a logarithmic divergency of the type: $\sum_{k=1}^{+\infty} 1/k$. For example, in this limit $r_3 \rightarrow R$ (3.4) has the following asymptotic behavior:

$$\varphi_4(r_3) \approx -\frac{G_N m}{R} \left[1 - \frac{a}{2\pi R} \ln \left(\frac{2\pi|R-r_3|}{a} \right) \right] \equiv -\frac{G_N m}{R} [1 + \delta], \quad (3.5)$$

where we took into account $R \gg a$ and $|R-r_3| \ll a$. In particular case $2\pi R = 10\text{cm}$ and $2\pi|R-r_3| = 10^{-1}a$, the deviation δ constitutes 2.3×10^{-3} and 2.3×10^{-18} parts of the newtonian value $-G_N m/R$ for $a = 10^{-2}\text{cm}$ and $a = 10^{-17}\text{cm}$, respectively. In principle, the former estimate is not very small. However, it is very difficult to set an experiment which satisfies the condition $|R-r_3| \ll a$. If the shell has a finite thickness, then the divergence disappears.

3.2. Spherical shell

Here, we consider a spherical shell of inner radius R_1 and outer radius R_2 and mass $m = 4\pi \int_{R_1}^{R_2} \rho(R) R^2 dR$ where $\rho(R)$ is a volume density of the shell (in the case of constant volume density $\rho = m / [\frac{4\pi}{3}(R_2^3 - R_1^3)]$). Then, the potential outside of the shell is

$$\begin{aligned} \varphi_D(r_3) &= -\frac{2G_N}{r_3} \left\{ \sum_k \frac{1}{\chi_k} e^{-2\pi\chi_k r_3} \int_{R_1}^{R_2} \rho(R) R \sinh(2\pi\chi_k R) dR \right\} \\ &\equiv \varphi_D^{(1)}(r_3), \quad r_3 > R_2, \end{aligned} \quad (3.6)$$

which for the constant ρ reads

$$\varphi_D(r_3) = -\frac{G_N m}{r_3} - \frac{G_N \rho}{2\pi^2 r_3} \sum_k' \frac{1}{\chi_k^3} \exp[-2\pi\chi_k r_3] h_k(R) \Big|_{R_1}^{R_2}, \quad (3.7)$$

where

$$h_k(R) = 2\pi\chi_k R \cosh[2\pi\chi_k R] - \sinh[2\pi\chi_k R]. \quad (3.8)$$

Inside of the shell we obtain:

$$\begin{aligned} \varphi_D(r_3) &= -\frac{2G_N}{r_3} \left\{ \sum_k \frac{1}{\chi_k} \sinh(2\pi\chi_k r_3) \int_{R_1}^{R_2} \rho(R) R e^{-2\pi\chi_k R} dR \right\} \\ &\equiv \varphi_D^{(2)}(r_3), \quad r_3 < R_1 \end{aligned} \quad (3.9)$$

and for the constant ρ :

$$\begin{aligned} \varphi_D(r_3) &= -2\pi G_N \rho (R_2^2 - R_1^2) \\ &+ \frac{G_N \rho}{\pi r_3} \sum_k' \frac{1}{\chi_k^2} \sinh(2\pi\chi_k r_3) \left[\left(R + \frac{1}{2\pi\chi_k} \right) e^{-2\pi\chi_k R} \right]_{R_1}^{R_2}. \end{aligned} \quad (3.10)$$

To get potential within the shell, we can use the following relation:

$$\varphi_D(r_3) = \varphi_D^{(1)}(r_3 | R_2 = r_3) + \varphi_D^{(2)}(r_3 | R_1 = r_3), \quad R_1 \leq r_3 \leq R_2. \quad (3.11)$$

Thus, in the case of constant ρ the gravitational potential within the shell reads

$$\begin{aligned} \varphi_D(r_3) &= 2\pi G_N \rho \left(\frac{r_3^2}{3} - R_2^2 + \frac{2R_1^3}{3r_3} \right) - \frac{G_N \rho}{2\pi^2 r_3} \sum_k' \frac{1}{\chi_k^3} \\ &\times [2\pi\chi_k r_3 - \sinh(2\pi\chi_k r_3) (2\pi\chi_k R_2 + 1) e^{-2\pi\chi_k R_2} - e^{-2\pi\chi_k r_3} h_k(R_1)]. \end{aligned} \quad (3.12)$$

For one extra dimension $d = 1$ we obtain a compact expression which is valid for full range of variable $r_3 \geq 0$:

$$\varphi_4(r_3) = -\frac{G_N \rho a}{r_3} \int_{R_1}^{R_2} R \ln \left\{ \frac{\cosh\left(\frac{2\pi(R+r_3)}{a}\right) - 1}{\cosh\left(\frac{2\pi(R-r_3)}{a}\right) - 1} \right\} dR, \quad (3.13)$$

where ρ is taken to be constant.

It can be easily seen that all these potentials are finite in the limit $r_3 \rightarrow R_1, R_2$ and $R_1 \neq R_2$, i.e. divergency of the potential is absent for finite thickness of the shell. However, divergency takes place for acceleration of a test body. We can see it from exact formulas for acceleration outside of the shell:

$$\begin{aligned} -\frac{d\varphi_D}{dr_3} &= -\frac{G_N m}{r_3^2} \\ &- \frac{G_N \rho}{2\pi^2 r_3^2} \sum_k' \frac{1}{\chi_k^3} (2\pi\chi_k r_3 + 1) e^{-2\pi\chi_k r_3} [h_k(R_2) - h_k(R_1)] < 0, \quad r_3 > R_2, \end{aligned} \quad (3.14)$$

within the shell:

$$\begin{aligned} -\frac{d\varphi_D}{dr_3} &= -\frac{4}{3}\pi G_N \rho \frac{r_3^3 - R_1^3}{r_3^2} \\ &- \frac{G_N \rho}{2\pi^2 r_3^2} \sum_k' \frac{1}{\chi_k^3} \{ h_k(r_3) (2\pi\chi_k R_2 + 1) e^{-2\pi\chi_k R_2} \\ &- (2\pi\chi_k r_3 + 1) e^{-2\pi\chi_k r_3} h_k(R_1) \}, \quad R_1 < r_3 < R_2 \end{aligned} \quad (3.15)$$

and inside of the shell:

$$-\frac{d\varphi_D}{dr_3} = -\frac{G_N\rho}{\pi r_3^2} \sum_k' \frac{1}{\chi_k^2} h_k(r_3) \left[\left(R + \frac{1}{2\pi\chi_k} \right) e^{-2\pi\chi_k R} \right]_{R_1}^{R_2} \geq 0, \quad r_3 < R_1. \quad (3.16)$$

All of these equations (3.14)-(3.16) have logarithmic divergency in the limit $r_3 \rightarrow R_1, R_2$, e.g. in $d = 1$ case:

$$-\frac{d\varphi_4}{dr_3} \longrightarrow \mp 2G_N\rho a \ln \frac{2\pi|R_{1,2} - r_3|}{a}, \quad (3.17)$$

where sign "−" corresponds to $r_3 \rightarrow R_1$ and sign "+" corresponds to $r_3 \rightarrow R_2$.

Putting the limit $R_1 \equiv 0, R_2 \equiv R$ in expressions obtained above in this subsection, we can get the corresponding equations for a sphere. For example, using the same conditions as for (3.5), we can get for a sphere ($d = 1$):

$$-\frac{d\varphi_4}{dr_3} \approx -\frac{G_N m}{R^2} \left[1 - \frac{3a}{2\pi R} \ln \left(\frac{2\pi|R - r_3|}{a} \right) \right] \equiv -\frac{G_N m}{R} [1 + \bar{\delta}]. \quad (3.18)$$

Therefore, deviation from the newtonian acceleration $\bar{\delta} = 3\delta$ and we can conclude that this deviation is also difficult to observe at experiments for considered parameters.

(3.14) and (3.16) show that acceleration changes the sign from negative outside of the shell to positive inside of the shell (see Figure 3). This change happens within the shell.

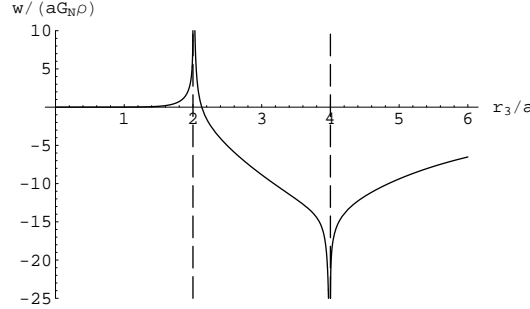


Figure 3. Graph of acceleration $w = -d\varphi_4/dr_3$ in dimensionless units (see (3.14)-(3.16)). Here, $a = 2.5, R_1 = 5$ and $R_2 = 10$. The dashed lines correspond to radii of the shell. The rightmost line goes to the newtonian asymptote $-1/r_3^2$ when $r_3 \rightarrow +\infty$. Point $r_3 = 0$ corresponds to unstable equilibrium.

3.3. Gravitational self-energy

Gravitational self-energy of the spherical shell with potential $\varphi_D(r_3)$ given by formulas (3.12) and (3.13) reads

$$U = 2\pi\rho \int_{R_1}^{R_2} r_3^2 \varphi_D(r_3) dr_3 = \frac{3G_N m^2}{10(R_2^3 - R_1^3)^2} (-2R_2^5 - 3R_1^5 + 5R_1^3 R_2^2) - \frac{9G_N m^2}{2(R_2^3 - R_1^3)^2} \sum_k' \frac{1}{(2\pi\chi_k)^2} \left[\frac{1}{3}(R_2^3 - R_1^3) + \frac{1}{(2\pi\chi_k)^3} E_k \right], \quad (3.19)$$

where

$$E_k = (1 + 2\pi\chi_k R_2)e^{-2\pi\chi_k R_2} [-h_k(R_2) + 2h_k(R_1)] - (1 + 2\pi\chi_k R_1)e^{-2\pi\chi_k R_1} h_k(R_1). \quad (3.20)$$

In the case of sphere $R_1 = 0, R_2 \equiv R$ and this expression is reduced to the following formula:

$$U = -\frac{3G_N m^2}{5R} \left\{ 1 + \frac{15}{2(2\pi R)^3} \times \sum_k' \frac{1}{\chi_k^3} \left[\frac{2\pi\chi_k R}{3} - \left(\frac{1}{2\pi\chi_k R} \right)^2 (1 + 2\pi\chi_k R)e^{-2\pi\chi_k R} h_k(R) \right] \right\} \equiv U_N + \delta U. \quad (3.21)$$

Here, U_N and δU are the newtonian self-energy of the sphere and deviation from it, respectively. In the case of one extra-dimension $d = 1$ and for condition $a \ll R$ we obtain:

$$\delta U \approx U_N \frac{5}{4\pi^2} \left(\frac{a}{R} \right)^2 \sum_{k=1}^{+\infty} \frac{1}{k^2} = U_N \frac{5}{24} \left(\frac{a}{R} \right)^2, \quad (3.22)$$

where we used that $\sum_{k=1}^{+\infty} 1/k^2 = \pi^2/6$. It is worth of noting that the correction to the newtonian formula has power law suppression instead of exponential one as it is usually expected in Kaluza-Klein models. Nevertheless, for astrophysical objects this correction term is negligibly small because of big difference between a and R . For example, if $a = 10^{-2}\text{cm}$, we get that $\delta U \approx 4 \times 10^{-27}U_N$ and $\delta U \approx 4 \times 10^{-19}U_N$ for Sun ($R \approx 7 \times 10^{10}\text{cm}$) and neutron star ($R \approx 7 \times 10^6\text{cm}$), respectively.

4. Gravitational interaction of two spherical shells

Let us consider two spherical shell with radiuses $R_1 < R_2$ and constant density ρ for first shell and radiuses $R'_1 < R'_2$ and constant density ρ' for second shell. Then, potential energy of gravitational interaction between these shells reads

$$U(r_3) = \int \int \int \varphi_D(r'_3) \rho' dV'. \quad (4.1)$$

Here, $r_3 \geq R_2 + R'_2$ is magnitude of three-dimensional vector between centers of shells and r'_3 is magnitude of three-dimensional vector between center of the first shell and an arbitrary elementary mass $dm' = \rho' dV'$ within second shell. Potential $\varphi_D(r'_3)$ is given by Eq. (3.7). After integration, we obtain:

$$U(r_3) = -\frac{G_N m m'}{r_3} - \frac{G_N \rho \rho'}{4\pi^4 r_3} \times \sum_k' \frac{1}{\chi_k^6} e^{-2\pi\chi_k r_3} [h_k(R_2) - h_k(R_1)][h_k(R'_2) - h_k(R'_1)]. \quad (4.2)$$

In the case of two spheres ($R_1 \equiv 0, R_2 \equiv R$ and $R'_1 \equiv 0, R'_2 \equiv R'$), this formula is reduced to:

$$U(r_3) = -\frac{G_N m m'}{r_3} - \frac{G_N \rho \rho'}{4\pi^4 r_3} \sum_k' \frac{1}{\chi_k^6} e^{-2\pi\chi_k r_3} h_k(R) h_k(R'). \quad (4.3)$$

4.1. Yukawa approximation

For working approximation, it is often sufficient to keep in sums the first Kaluza-Klein modes, i.e. to use the Yukawa approximation. In this approximation, (4.2) and (4.3) can be rewritten correspondingly:

$$U(r_3) \approx -\frac{G_N m m'}{r_3} - \frac{16\pi^2 G_N \rho \rho' \alpha \lambda^6}{r_3} e^{-r_3/\lambda} \tilde{h}(R)|_{R_1}^{R_2} \tilde{h}(R)|_{R'_1}^{R'_2} \quad (4.4)$$

and

$$U(r_3) \approx -\frac{G_N m m'}{r_3} \left[1 + 9\alpha \left(\frac{\lambda}{R} \right)^3 \left(\frac{\lambda}{R'} \right)^3 e^{-r_3/\lambda} \right] \tilde{h}(R) \tilde{h}(R'), \quad (4.5)$$

where

$$\tilde{h}(R) = \frac{R}{\lambda} \cosh\left(\frac{R}{\lambda}\right) - \sinh\left(\frac{R}{\lambda}\right). \quad (4.6)$$

Here, $\lambda = a/(2\pi)$ and parameter $\alpha = 2s$ is described in (2.9).

4.2. Gravitational force between two spheres

In Yukawa approximation, gravitational force between two spheres is

$$\begin{aligned} F(r_3) &= -\frac{dU}{dr_3} \approx -\frac{G_N m m'}{r_3^2} \left[1 + 9\alpha \left(\frac{\lambda}{R} \right)^3 \left(\frac{\lambda}{R'} \right)^3 \frac{r_3}{\lambda} e^{-r_3/\lambda} \right] \tilde{h}(R) \tilde{h}(R') \\ &\approx -\frac{G_N m m'}{r_3^2} \left[1 + \frac{9}{4}\alpha \left(\frac{\lambda}{R} \right)^2 \left(\frac{\lambda}{R'} \right)^2 \frac{r_3}{\lambda} e^{-(r_3-R-R')/\lambda} \right], \end{aligned} \quad (4.7)$$

where in the last expression we use conditions $R, R' \gg \lambda$. If surfaces of the spheres are on the distances of the order of the maximal period: $r_3 - R - R' \sim a$, then we get

$$F(r_3) \approx -\frac{G_N m m'}{r_3^2} \left[1 + 0.0084s \left(\frac{\lambda}{R} \right)^2 \left(\frac{\lambda}{R'} \right)^2 \frac{r_3}{\lambda} \right] \equiv -\frac{G_N m m'}{r_3^2} (1 + \tilde{\delta}). \quad (4.8)$$

For example, in the case of one extra dimension and $R = R' = 1\text{cm}$, $\lambda = 4.7 \times 10^{-3}\text{cm}$, we get for deviation from the newtonian formula the estimate $\tilde{\delta} = 1.8 \times 10^{-9}$. To obtain it, it is necessary to remember that for $d = 1$ parameter $s = 1$.

5. Smeared extra dimensions

Now, we get onto the asymmetrical extra dimension models (cf. with [8]) with topology

$$M_D = \mathbb{R}^3 \times T^{d-p} \times T^p, \quad p \leq d, \quad (5.1)$$

where we suppose that $(d-p)$ tori have the same "large" period a and p tori have "small" equal periods b . In this case, the fundamental Planck scale relation (2.5) reads

$$\frac{S_D}{S_3} \cdot M_{Pl(4)}^2 = M_{Pl(D)}^{2+d} a^{d-p} b^p. \quad (5.2)$$

Additionally, we assume that test bodies are uniformly smeared/spreaded over small extra dimensions. Thus, test bodies have a finite thickness in small extra dimensions (thick brane approximation). For short, we shall call such small extra dimensions as "smeared" extra dimensions. If $p = d$ then all extra dimensions are smeared.

It is not difficult to show that the gravitational potential does not feel smeared extra dimensions. We can prove this statement by three different methods. First, we can directly solve D-dimensional Poisson equation (2.1) with the periodic boundary conditions for the extra dimensions ξ_{p+1}, \dots, ξ_d and the mass density $\rho = (m / \prod_{i=1}^p a_i) \delta(\mathbf{r}_3) \delta(\xi_{p+1}) \dots \delta(\xi_d)$. As a result, we obtain the unique solution $\varphi_D(\mathbf{r}_3, \xi_{p+1}, \dots, \xi_d)$ of the form (2.3) which does not depend on ξ_1, \dots, ξ_p and satisfies the limit $\lim_{r_3 \rightarrow +\infty} \varphi_D(\mathbf{r}_3, \xi_{p+1}, \dots, \xi_d) = 0$.

Second, we can average solutions (2.3) (where point mass m is replaced by $m \prod_{i=1}^p (d\xi_i/a_i)$) over smeared dimensions ξ_1, \dots, ξ_p and take into account that $\int_0^a \cos(2\pi k\xi/a) d\xi = 0, a$ for $k \neq 0$ and $k = 0$, respectively. Thus, the terms with these variables disappear from (2.3). For example, direct integration of the compact expression (2.7) results in pure newtonian formula:

$$\begin{aligned} & -\frac{G_N m}{ar_3} \sinh\left(\frac{2\pi r_3}{a}\right) \int_0^a \left[\cosh\left(\frac{2\pi r_3}{a}\right) - \cos\left(\frac{2\pi \xi}{a}\right) \right]^{-1} d\xi \\ &= -\frac{G_N m}{\pi r_3} \arctan \left[\left(\frac{\cosh\left(\frac{2\pi r_3}{a}\right) + 1}{\cosh\left(\frac{2\pi r_3}{a}\right) - 1} \right)^{1/2} \tan\left(\frac{\pi \xi}{a}\right) \right]_0^a = -\frac{G_N m}{r_3}. \end{aligned} \quad (5.3)$$

Finally, from the symmetry of the model, it is clear that in the case of a test mass smeared over extra dimensions, the gravitational field vector $\mathbf{E}_D = -\nabla_D \varphi_D$ does not have components with respect to smeared extra dimensions. For example, if we consider the model with topology of a cylinder $S^1 \times \mathbb{R}$ where S^1 is the smeared extra dimension and \mathbb{R} is the external dimension, then \mathbf{E}_2 will be parallel to an element of the cylinder. For simplicity, let us consider a model where all extra dimensions are smeared. Then, the Poisson equation (2.1) can be rewritten in the form:

$$\nabla_D \mathbf{E}_D = -S_D G_D \rho_D(\mathbf{r}_D) = -4\pi G_N m \delta(\mathbf{r}_3), \quad (5.4)$$

where we use relation (2.4) between gravitational constants and formula $\rho_D(\mathbf{r}_D) = m\delta(\mathbf{r}_3) / \prod_{i=1}^d a_i$. After integrating both parts of this formula over multidimensional volume $V = V_3 \cup V_{internal}$ we obtain:

$$\int_V E_D^{\alpha_i},_{\alpha_i} d^D V = -4\pi G_N m V_{internal} = \text{const}. \quad (5.5)$$

Here, $d^D V = \varepsilon_{|\alpha_1, \dots, \alpha_D|} dx^{\alpha_1} \wedge \dots \wedge dx^{\alpha_D} = dx dy dz dx^{i_1} \dots dx^{i_d}$ and $\alpha_i = 1, 2, 3, i_1, \dots, i_d$. Indexes i_1, \dots, i_d enumerate extra dimensions. Applying the Gauss theorem, we get

$$\int_V E_D^{\alpha_i},_{\alpha_i} d^D V = \int_{\partial V} E_D^{\alpha_i} d^{D-1} \Sigma_{\alpha_i} = 4\pi R_3^2 E_D V_{internal}, \quad (5.6)$$

where

$$d^{D-1} \Sigma_{\alpha_i} = \varepsilon_{\alpha_i |\alpha_j \dots \alpha_k|} \underbrace{dx^{\alpha_j} \wedge \dots \wedge dx^{\alpha_k}}_{D-1} \quad (5.7)$$

and in three-dimensional spherical coordinates $d^{D-1} \Sigma_{r_3} = R_3^2 \sin \vartheta d\vartheta d\varphi dx^{i_1} \dots dx^{i_{D-3}}$. To get (5.6), we use the fact that $E_D^{r_3} \equiv E_D$ is the only non-zero component of the gravitational field vector. Therefore, comparing (5.5) and (5.6), we obtain:

$$E_D(r_3) = -\frac{G_N m}{r_3^2} \implies \varphi_D(r_3) = -\frac{G_N m}{r_3}. \quad (5.8)$$

Thus, all these 3 approaches show that the gravitational potential does not feel smeared extra dimensions. It means that in the case of p smeared extra dimensions, the wave numbers k_1, \dots, k_p disappear from (2.3) and we should perform summation only with respect to k_{p+1}, \dots, k_d .

5.1. Effective gravitational constant

As it follows from (4.7), in the Yukawa approximation, the gravitational force between two spheres with masses m_1, m_2 , radiuses R_1, R_2 and distance r_3 between the centers of the spheres reads:

$$F(r_3) = -\frac{G_{N(eff)}(r_3)m_1m_2}{r_3^2}, \quad (5.9)$$

where

$$\begin{aligned} G_{N(eff)}(r_3) &\approx G_N \left\{ 1 + \frac{9}{2}(d-p) \left(\frac{\lambda}{R_1} \right)^2 \left(\frac{\lambda}{R_2} \right)^2 \frac{r_3}{\lambda} e^{-(r_3-R_1-R_2)/\lambda} \right\} \\ &\equiv G_N(1 + \delta_G) \end{aligned} \quad (5.10)$$

is an effective gravitational constant. Here, we took into account that in the case of p smeared dimensions, the prefactor α should be replaced by $2(d-p)$. Now, we want to evaluate the corrections δ_G to the Newton's gravitational constant and to estimate their possible influence on the experimental data. As it follows from Figure 2 in the CODATA 2006, the most precise values of G_N were obtained in the University Washington and the University Zürich experiments [9, 10]. They are $G_N/10^{-11}\text{m}^3\text{kg}^{-1}\text{s}^{-2} = 6.674215 \pm 0.000092$, and 6.674252 ± 0.000124 , respectively. Let us consider two particular examples: ($\mathcal{D} = 5$)-dimensional model with $d = 1, p = 0 \rightarrow \alpha = 2$ and ($\mathcal{D} = 10$)-dimensional model with $d = 6, p = 3 \rightarrow \alpha = 6$. For these values of α , Figure 6 in [7] gives the upper limits for $\lambda = a/(2\pi)$ correspondingly $\lambda \approx 4.7 \times 10^{-3}\text{cm}$ and $\lambda \approx 3.4 \times 10^{-3}\text{cm}$. To calculate δ_G , we take parameters of the Moscow experiment [11]: $R_1 \approx 0.087\text{cm}$ for a platinum ball with the mass $m_1 = 59.25 \times 10^{-3}\text{g}$, $R_2 \approx 0.206\text{cm}$ for a tungsten ball with the mass $m_2 = 706 \times 10^{-3}\text{g}$ and $r_3 = 0.3773\text{cm}$. For both of these models we obtain $\delta_G \approx 8.91 \times 10^{-12}$ and $\delta_G \approx 1.06 \times 10^{-14}$, respectively. These values are rather far from the measurement accuracy of G_N in [9, 10]. In future, if we can achieve in the Moscow-type experiments the accuracy within these values, then, changing radii $R_{1,2}$ and distance r_3 , we can reveal extra dimensions or obtain experimental limitations on considered models. We should note that small changes in experimental bounds for λ result in drastic changes of δ_G . For example, if for λ we take the upper limits $\lambda \approx 2 \times 10^{-2}\text{cm}$ and $\lambda \approx 1.3 \times 10^{-2}\text{cm}$ which follow from previous experiments (see Figure 5 in [1] for $\alpha = 2$ and 6, respectively) then $\delta_G \approx 0.0006247$ and $\delta_G \approx 0.0000532$ and these figures are very close to the measurement accuracy of G_N in [9, 10].

5.2. Model: $\mathcal{D} = 10$ with $d = 6, p = 3$

Let us consider in more detail ($\mathcal{D} = 10$)-dimensional model with 3 smeared dimensions. Here, we have very symmetrical with respect to a number of spacial dimensions structure: 3 our external dimensions, 3 large extra dimensions with periods a and 3 small smeared extra dimensions with periods b . For b we put a limitation: $b \leq b_{max} = 10^{-17}\text{cm}$ which is usually taken for thick brane approximation. This

limitation follows from the electrical inverse-square law experiments. Although, in the next subsection we show that such approach can be significantly relaxed for models with smeared extra dimension, here we still use this bound.

As we mentioned above, in the case of $\alpha = 6$, for a we should take a limitation $a \leq a_{max} = 2.1 \times 10^{-2} \text{cm}$. To solve the hierarchy problem, the multidimensional Planck scale is usually considered from 1TeV up to approximately 130 TeV (see e.g. [8, 12]). To make some estimates, we take $M_{min} = 1\text{TeV} \lesssim M_{Pl(10)} \lesssim M_{max} = 50\text{TeV}$. Thus, as it follows from (5.2), the allowed values of a and b should satisfy inequalities:

$$\frac{S_9}{S_3} \frac{M_{Pl(4)}^2}{M_{max}^8} \leq a^3 b^3 \leq \frac{S_9}{S_3} \frac{M_{Pl(4)}^2}{M_{min}^8}. \quad (5.11)$$

Counting all limitations, we find allowed region for a and b (shadow area in Figure 4). In this trapezium, the upper horizontal and right vertical lines are the decimal logarithms of a_{max} and b_{max} , respectively. The right and left inclined lines correspond to $M_{Pl(10)} = 1\text{TeV}$ and $M_{Pl(10)} = 50\text{TeV}$, respectively. To illustrate this picture, we consider two points A and B on the line $M_{Pl(10)} = 1\text{TeV}$. Here, we have $a = 2.1 \times 10^{-2} \text{cm}$, $b = 10^{-20.9} \text{cm}$ for A and $a = 10^{-4} \text{cm}$, $b = 10^{-18.6} \text{cm}$ for B. These values of large extra dimensions a are much bigger than in the standard approach $a \sim 10^{(32/6)-17} \text{cm} \approx 10^{-11.7} \text{cm}$ [2, 3].

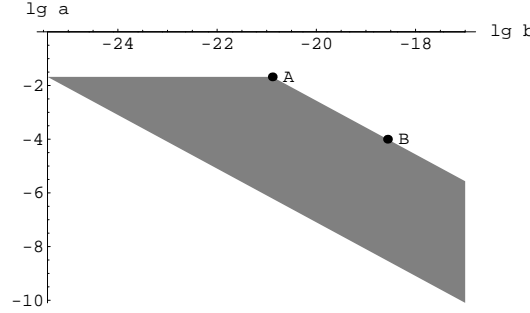


Figure 4. Allowed region (shadow area) for periods of large (a) and smeared (b) dimensions in the model $\mathcal{D} = 10$ with $d = 6, p = 3$.

5.3. Model: \mathcal{D} -arbitrary and $d = p$

In this model, the test masses are smeared over all extra dimensions. Therefore, in non-relativistic limit, there is no deviation from the Newton's law at all. Surprisingly, this result does not depend on the size of smeared extra dimensions. The ISL experiments will not show any deviation from the Newton's law without regard to the size b (see also (5.10) where $d - p = 0$). Similar reasoning are also applicable to Coulomb's law. It is necessary to suggest other experiments which can reveal the multidimensionality of our spacetime. Nevertheless, we can solve the hierarchy problem in this model because (5.2) (where $d = p$) still works. For example, in the case of bosonic string dimension $\mathcal{D} = 26$ we find $M_{Pl(26)} \approx 31\text{TeV}$ for $b = 10^{-17} \text{cm}$. In the case $\mathcal{D} = 10$ we get $M_{Pl(10)} \approx 30\text{TeV}$ for $b = 5.59 \times 10^{-14} \text{cm}$. In general, if we suppose that $1\text{TeV} \lesssim M_{Pl(\mathcal{D})} \lesssim 30\text{TeV}$ then we obtain:

$$p = 1, \quad 1.65 \times 10^{11} \text{cm} \lesssim b \lesssim 4.46 \times 10^{15} \text{cm},$$

$$\begin{aligned}
p = 2, \quad & 3.81 \times 10^{-4} \text{cm} \lesssim b \lesssim 3.43 \times 10^{-1} \text{cm}, \\
p = 3, \quad & 4.83 \times 10^{-9} \text{cm} \lesssim b \lesssim 1.40 \times 10^{-6} \text{cm}, \\
& \vdots \\
p = 6, \quad & 5.59 \times 10^{-14} \text{cm} \lesssim b \lesssim 5.21 \times 10^{-12} \text{cm},
\end{aligned}$$

where lower limit corresponds to 30TeV and upper limit agrees with 1TeV.

6. Conclusions

We have considered generalization of the Newton's potential to the case of extra dimensions where multidimensional space has topology $M_D = \mathbb{R}^3 \times T^d$. We obtained the exact solution (2.3) which describes smooth transition from the newtonian behavior $1/r_3$ for distances bigger than periods of tori (the extra dimension sizes) to multidimensional behavior $1/r_{3+d}^{1+d}$ in opposite limit. In the case of one extra dimension, the gravitational potential is expressed via compact and elegant formula (2.7). We applied these exact solutions to some practical problems to get the gravitational potentials for considered configurations. Found potentials were used to calculate the acceleration for point masses and gravitational self-energy.

To estimate corrections to the newtonian expressions, it is sufficient to keep only the first Kaluza-Klein modes. Then, we obtained that the correction term has the form of the Yukawa potential with parameters defined by multidimensional models. Such representation gave us a possibility to use the results of the inverse square-law experiments to get limitations on periods of tori. As an Yukawa potential approximation, it was shown that in the Cavendish-type experiments the corrections (due to the extra dimensions) to the newtonian gravitational constant are still far from the measurement accuracy of experiments for the determination of G_N .

Then, we proposed models where test masses can be smeared over the extra dimensions. The number of the smeared dimensions can be equal or less than the total number of the extra dimensions. We proved that the gravitational potential does not feel the smeared dimensions and this conclusion does not depend on the size of these dimensions. Such approach opens new remarkable possibilities. For example in the case $\mathcal{D} = 10$ with 3 large and 3 smeared extra dimensions and $M_{Pl(10)} = 1\text{TeV}$, the large extra dimensions can be as big as the upper limit established by the ISL experiments for $\alpha = 6$, i.e. $a \approx 2.1 \times 10^{-2}\text{cm}$. This value of a is in many orders of magnitude bigger than the rough estimate $a \approx 10^{-11.7}\text{cm}$ obtained from the fundamental Planck scale relation of the usual form (2.5). The limiting case where all extra dimensions are smeared is another interesting example. Here, there is no deviation from the Newton's law at all. Thus, these models can explain negative results for the detection of the extra dimensions in ISL experiments irrespective of the size of the extra dimensions. Nevertheless, these models can be still used to solve the hierarchy problem.

Acknowledgments

We thank Uwe Günther for his stimulating discussions. A. Zh. acknowledges the hospitality of the Theory Division of CERN and the High Energy, Cosmology and Astroparticle Physics Section of the ICTP during preparation of this work. This work

was supported in part by the "Cosmomicrophysics" programme of the Physics and Astronomy Division of the National Academy of Sciences of Ukraine.

Appendix A. The gravitational force law under dimensional reduction

Let us consider a product space M_D consisting of two components $M_D = M_3 \times M_d$, where for simplicity of the subsequent calculations we assume $M_3 = \mathbb{R}^3$ as 3-dimensional flat external space and a d -torus $M_d = T^d$ (with the same characteristic length a along each of the d dimensions) as compact internal space. The volume of M_d is hence given as $\text{vol}(M_d) = V_d = a^d$.

The aim of this appendix is to demonstrate that the force laws for the full theory on M_D and the effective theory on M_3 have correspondingly the form

$$F(r_{3+d}) = G_{\mathcal{D}} \frac{m_1 m_2}{r_{3+d}^{2+d}}, \quad (\text{A.1})$$

$$F(r_3) = G_N \frac{m_1 m_2}{r_3^2}, \quad (\text{A.2})$$

where gravitational constants $G_{\mathcal{D}}$ and G_N are related with each other in accordance with (2.4). To perform it, we consider separately the regimes of small distances $r_{3+d} \ll a$ compared to the size of the internal space and of large distances $r_3 \gg a$. For $r_{3+d} \ll a$ the field lines penetrate all D space dimensions, whereas at length scales $r_3 \gg a$ the internal dimensions are not accessible and effectively the field lines are spreading only along the 3 spatial dimensions of the external space M_3 .

As in [3], we pass for simplicity of the calculations from the compact d -torus to its covering space \mathbb{R}^d . The single mass m_1 in T^d is then mapped to a mass lattice in \mathbb{R}^d , which is build from m_1 and its mirror images in the cover.

For a test mass m_2 at a small distances $r_{3+d} \ll a$ from m_1 the mirror masses give a negligible contribution to the gravitational force and in first order approximation the Gauss law in D space dimensions holds in accordance with (A.1). In this case the infinite set of mirror masses can in rough approximation be considered as symmetrically distributed around m_1 , m_2 so that their contributions will compensate each other.

For the analysis of the opposite case of a large separation $r_3 \gg a$ between the masses m_1 and m_2 , we assume the mass m_1 placed in the origin of the D -dimensional space. The lattice of the mirror masses spans then a d -dimensional subspace \mathbb{R}^d ("wire") in the space $\mathbb{R}^d \times \mathbb{R}^3$ and the total effective force F_{eff} will result from the gravitational attraction of the whole lattice-subspace. For $r_3 \gg a$, the mirror masses appear homogeneously smeared about this subspace with a "surface" density m_1/a^d . Let us choose coordinates

$$(\mathbf{z}, \mathbf{r}_3) \in \mathbb{R}^d \times \mathbb{R}^3 \quad (\text{A.3})$$

and a test mass m_2 located at the point $(0, \mathbf{r}_3)$. The force orthogonal to the lattice produced on m_2 by a small volume element dV_d at a point $(\mathbf{z}, 0)$ of the (lattice) covering space \mathbb{R}^d is given by

$$\begin{aligned} dF(z, r_3) &= G_{\mathcal{D}} \frac{r_3}{(z^2 + r_3^2)^{1/2}} \frac{m_1 dV_d}{a^d} \frac{m_2}{(z^2 + r_3^2)^{(2+d)/2}} \\ &= \frac{G_{\mathcal{D}} m_1 m_2}{a^d} \frac{r_3 dV_d}{(z^2 + r_3^2)^{(3+d)/2}}. \end{aligned} \quad (\text{A.4})$$

The factor $r_3/(z^2 + r_3^2)^{1/2}$ is the cosine between the force direction and the lattice normal. Due to the lattice symmetry, the force component parallel to the lattice is compensated by an opposite force component from the point $(-\mathbf{z}, 0)$. The total effective force $F_{eff}(r_3)$ of the mass lattice on the test particle can now be easily obtained by integrating over the volume of \mathbb{R}^d . Choosing spherical coordinates on \mathbb{R}^d , the volume of a thin shell with radius z is

$$dV_d = S_d z^{d-1} dz, \quad (\text{A.5})$$

where S_d is square of $(d-1)$ -dimensional sphere of a unit radius (see (2.1)) and the total effective force can be calculated as

$$F_{eff}(r_3) = \frac{G_{\mathcal{D}} m_1 m_2}{a^d} r_3 S_d \int_0^\infty \frac{z^{d-1} dz}{(z^2 + r_3^2)^{(3+d)/2}}. \quad (\text{A.6})$$

With the substitution $t = z^2$ the integral can be transformed to the standard integral [5]

$$\int_0^\infty \frac{x^{\alpha-1} dx}{(x+b)^\rho} = b^{\alpha-\rho} B(\alpha, \rho-\alpha), \quad 0 < \Re \alpha < \Re \rho \quad (\text{A.7})$$

so that for the corresponding term in (A.6) we find

$$\begin{aligned} \int_0^\infty \frac{z^{d-1} dz}{(z^2 + r_3^2)^{(3+d)/2}} &= \frac{1}{2} \int_0^\infty \frac{t^{d/2-1} dt}{(t + r_3^2)^{(3+d)/2}} \\ &= \frac{1}{2r_3^3} B\left(\frac{d}{2}, \frac{3}{2}\right) = \frac{1}{r_3^3} \frac{\Gamma(\frac{d}{2}) \Gamma(\frac{3}{2})}{2\Gamma(\frac{3+d}{2})}. \end{aligned} \quad (\text{A.8})$$

Expressing the Γ -functions in (A.8) in terms of surface areas: $\Gamma(D/2) = 2\pi^{D/2}/S_D$ gives

$$\int_0^\infty \frac{z^{d-1} dz}{(z^2 + r_3^2)^{(3+d)/2}} = \frac{1}{r_3^3} \frac{S_{3+d}}{S_d S_3}. \quad (\text{A.9})$$

Hence, the total effective force takes the simple form

$$F_{eff}(r_3) = \frac{G_{\mathcal{D}} S_{3+d}}{S_3 a^d} \frac{m_1 m_2}{r_3^2} \quad (\text{A.10})$$

and equating it with the gravitational force law (A.2) in three-dimensional space, we reproduce the result (2.4) for the relation between three-dimensional and multidimensional gravitational constants.

References

- [1] Adelberger E.G., Heckel B.R. and Nelson A.E. 2003 *Ann. Rev. Nucl. Part. Sci.* **53**, 77; arXiv:hep-ph/0307284.
- [2] Arkani-Hamed N., Dimopoulos S. and Dvali G. 1998 *Phys. Lett. B* **429**, 263; hep-ph/9803315. Antoniadis I., Arkani-Hamed N., Dimopoulos S. and Dvali G. 1998 *Phys. Lett. B* **436**, 257; arXiv:hep-ph/9804398.
- [3] Arkani-Hamed N., Dimopoulos S. and Dvali G. 1999 *Phys. Rev. D* **59**, 086004; arXiv:hep-ph/9807344.
- [4] Callin P. and Burgess C.P. 2006 *Nucl. Phys. B* **752**, 60; arXiv:hep-ph/0511216.
- [5] Prudnikov A.P., Brychkov Yu.A. and Marichev O.I. 1986 *Integrals and Series, vol. 1: Elementary Functions*, (New York: Gordon and Breach Science Publishers).
- [6] Barvinsky A.O. and Solodukhin S.N. 2003 *Nucl. Phys. B* **675**, 159; arXiv:hep-th/0307011.
- [7] Kapner D.J., Cook T.S., Adelberger E.G., Gundlach J.H., Heckel B.R., Hoyle C.D. and Swanson H.E. 2007 *Phys. Rev. Lett.* **98**, 021101; arXiv:hep-ph/0611184.

- [8] Lykken J. and Nandi S. 2000 *Phys. Lett. B* **485**, 224; arXiv:hep-ph/9908505.
- [9] Gundlach J.H. and Merkowitz S.M. 2000 *Phys. Rev. Lett.* **85**, 2869; arXiv:gr-qc/0006043.
- [10] Schlaminger St., Holzschuh E., Kündig W., Nolting F., Rixley R.E., Schurr J. and Straumann U. 2006 *Phys. Rev. D* **74**, 082001; arXiv:gr-qc/0609027.
- [11] Mitrofanov V.P. and Ponomareva O.I. 1988 *Sov. Phys. JETP* **67**, 1963.
- [12] Hannestad S. and Raffelt G. 2001 *Phys. Rev. Lett.* **87**, 051301; arXiv:hep-ph/0103201.